Sizing an Electrical Storage in Combination with Thermochemical Storage for a PVT-Driven Energy System in a Residential Application

Adriana Coca-Ortegón[1], Raquel Simón-Allué[1], Alberto Belda[2], Ismael Lozano[2], Georgios Martinopoulos[3], Alexandros Tsimpoukis[3], Nikolaos Nikolopoulos[3], Yolanda Lara[1]

[1] ENDEF Solar Solutions, Zaragoza (Spain)

[2] Fundación CARTIF, Valladolid (Spain)

[3] Centre for Research & Technology Hellas / Chemical Process and Energy Resources Institute, Thessaloniki (Greece)

Abstract

This work is focused on sizing electrical storage based on Li-ion batteries in combination with a thermochemical (TCM) storage for a system, driven by photovoltaic thermal (PVT) collectors coupled to a vapor compression heat pump, that provides heating, cooling, domestic hot water (DHW) and electricity in residential buildigs.

A sensitivity analysis of the electrical storage system is performed considering two sizes for the TCM storage to minimize the electrical requirement from the grid. The analysis is conducted through a simplified model implemented in the dynamic simulation software TRNSYS. This model uses as input the base electrical load profiles for the building and the TCM subsystem.

The electrical profiles linked to the TCM components are obtained from a more detailed model developed in Aspen and MATLAB, which considers the thermal loads in the building, and the internal TCM system configuration.

Keywords: Photovoltaic-Thermal collectors, PVT system, thermochemical storage, electrical storage

1. Introduction

Energy efficiency and the decarbonization of the building sector are the main objectives of energy policy worldwide. Currently, final energy consumption in buildings is mainly due to thermal uses, including space heating, water heating and cooking which represent 33%, 13% and 8%, respectively, followed by electrical appliances with a 16% share. Cooling is also a thermal use that currently represents 6% of overall final consumption, but this figure is expected to grow considerably by 2050, especially in developed countries (IEA, 2023a).

To achieve the energy policy objectives at European level, it is necessary to combine different strategies, such as the integration of renewable energies in buildings, the electrification of the thermal demand through efficient technologies such as heat pumps and the use of effective energy storage systems.

Among the renewable technology options, solar technology stands as one of the most promising for application at the building level, due to the ease of installation and integration. Particularly, the use of solar photovoltaic-thermal (PVT) technology has been growing in recent years (IEA, 2022), as it produces thermal and photovoltaic energy in a single device, with better overall efficiency than individual photovoltaic technology (Tiwari et al., 2023; Zondag, 2008).

The use of energy storage is also a key point to be included in the building energy systems' design. Within thermal storage technologies, the most common option used in buildings is sensible heat storage through water tanks (Fan and Luo, 2018; Koçak et al., 2020), followed by latent heat storage based on phase change materials (PCM) (Dincer and Rosen, 2011; Jouhara et al., 2020). Another thermal storage option with a higher energy density is the thermochemical (TCM) storage (Jarimi et al., 2019; Salgado-Pizarro et al., 2022), which is currently implemented in buildings mainly at the demonstration level. Electrical storage with electrochemical technology based on Li-ion batteries is another option that has been growing in the building sector in recent

Selection and/or peer review under responsibility of Scientific Committee
10.18086/eurosun.2024.02.04 Available at http://proceedings.ises.org

years linked to the increment of self-consumption PV installations. The Li-ion battery price is still high, although it is expected that costs will decrease, thereby gaining a more competitive position (Kebede et al., 2022; MI (Mordor Intelligence), 2022; Xu et al., 2022).

This paper focuses on the sizing of an electrical storage system (ESS) based on Li-ion batteries for two sizes of TCM storage (17.5 and 30 kWh). These energy storage technologies are integrated into a building energy system, driven by a PVT-solar system in combination with an air-to-water vapor compression heat pump (HP). This energy system will provide thermal and electrical energy to an 80 m^2 building located in Santiago de Compostela (Spain). The objective is to define suitable ESS sizes that minimize the electrical dependency on the grid.

2. Methodology

2.1 Overall system description

The energy system analyzed consists of three main systems: i) the PVT-HP energy generation system, in charge of producing electricity and thermal energy through a hybrid PVT solar field and an air source HP, including an ESS based on Li-ion batteries; ii) the MiniStor system, where the thermal energy is stored through a thermochemical (TCM) storage in combination with a small heat pump and phase change materials (PCM) vessels; iii) the building's demand, which is met using the existing energy generation system, as well as the energy supply from the MiniStor system. Figure 1 shows the overall energy system scheme.

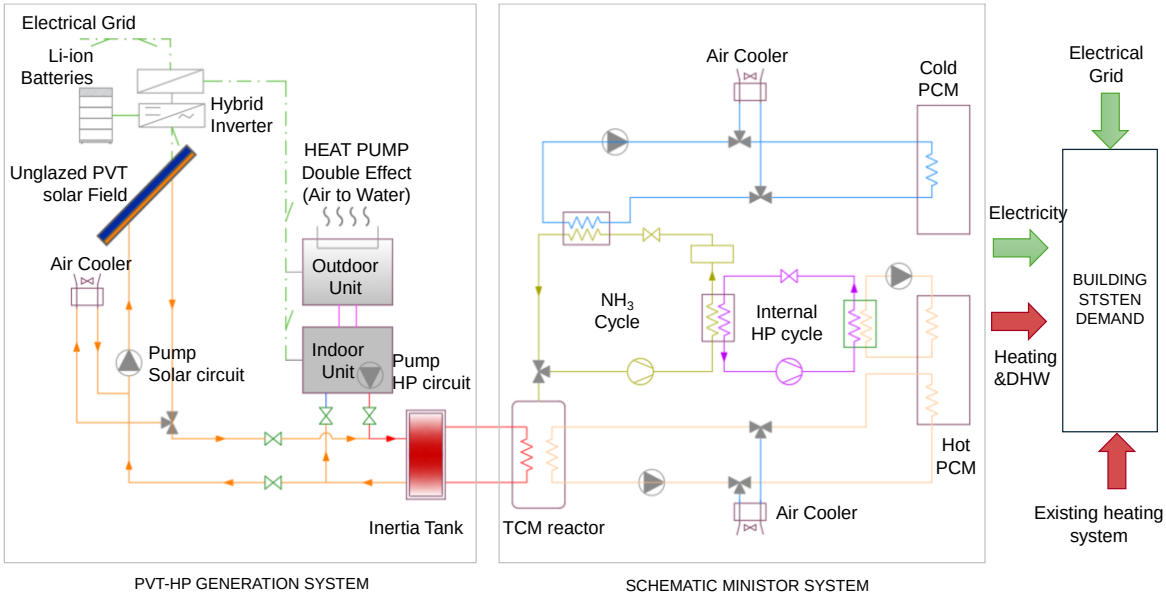

Fig. 1: Overall energy system scheme

The PVT-HP generation system includes a 39.2 m^2 solar field with unglazed liquid-based PVT collectors (nominal electrical power 7.80 kWp), which are hydraulically integrated, using a parallel configuration through an inertia tank (Lazzarin, 2020), with an air-to-water vapor compression HP (nominal capacity 11 kW in heating). The PVT electrical production is dedicated firstly to run the air-to water HP, with any excess being used to cover the building electrical demand or stored in the ESS. The PVT thermal production is used to pre-heat the inertia tank, which the air-to-water HP uses to provide thermal energy for the MiniStor system.

The MiniStor system included several subsystems: i) a TCM reactor containing ammoniated $CaCl_2$ salts, ii) an ammonia refrigeration cycle with a liquid ammonia storage tank, iii) a complementary small ammonia-to-water HP and iv) PCM units, through which the connection of MiniStor with the building is realized. (Tsimpoukis et al., 2024).

During the winter, in the TCM reactor operates by performing a solid-gas sorption process, that stores heat energy efficiently and at a high density. During the charging phase, it is used heat (44 to 70 °C) to produce a gaseous ammonia stream (NH_3) which is compressed, condensed and stored in a tank. Next, the condensation heat is used by the internal small heat pump, to charge a hot PCM vessel or cover the heating needs in the

building. During the discharging phase, the NH_3 stored as liquid in the tank is used. If the reactor equilibrium pressure is lower than the evaporation pressure, the material flows into the evaporator and evaporates at a temperature set by the surrounding environment. The gaseous ammonia is adsorbed in the reactor and since this is an exothermic reaction, the excess heat is used to cover the thermal demand.

During summer, the previous procedure is slightly modified. Because the heating thermal demand is negligible, the operation of the water-to-water HP during the charging phase is not necessary. The heat produced by the PVT-HP system is sufficient for covering the DHW loads, and thus the ammonia condensation heat is rejected to the ambient. The MiniStor system also provides cooling by exploiting the NH_3 evaporation, during the discharging mode; however, this effect is not required in the case of the analyzed building.

2.2 Energy demand estimation

The energy demand at the building includes the thermal loads (heating and DHW), as well as the electrical loads linked to the different lights and equipment used inside the building.

For the heating demand, a load profile is estimated following the EN 12831:2017 Standard (CEN and CENELEC, 2017) . The DHW demand is estimated following the Spanish Technical Building Code (Ministry of Development of Spain, 2019), which indicates that the average daily DHW demand in a residential building can be estimated at 28 liters per person produced at 60 °C. Considering the two previous reference norms and four people in the building, the overall thermal load profiles were defined for a typical day according to the season: extreme winter, average winter, autumn-spring and summer season.

The electrical demand considers three different load profiles: i) the electrical loads in the building, ii) the electrical loads of the air-to-water HP and iii) the electrical demand linked to the MiniStor system. The electrical load profile in the building was defined by studying the building inhabitant's behavior and monthly consumption data. The electrical load of the HP is obtained from a TRNSYS simulation model, by activating the equipment on a limited schedule during the day taking into consideration the average monthly PVT-electrical production. Finally, the load electrical profiles for the MiniStor system are obtained for defined typical days using a MATLAB/Simulink - ASPEN model, where the MiniStor system is modelled in detail (Zisopoulos et al., 2021).

2.3 Simulation model

The energy system that supplies thermal and electrical energy to the building is simulated using a simplified model implemented in the dynamic simulation software TRNSYS (SEL (Solar Energy Laboratory), 2018). This model has three main purposes, to simulate the PVT electrical and thermal production, to simulate the air-to-water HP thermal production as well as the corresponding electrical consumption, and finally to size the ESS. Internally the TRNSYS model included four main subsystems: (i) the PVT-HP generation subsystem, (ii) the electrical subsystem, (iii) the simplified thermal demand subsystem and (iv) the weather data subsystem. The implemented model is shown in Figure 2.

The PVT-HP generation sub-system includes the PVT solar field with the solar loop as well as the air-source HP with the corresponding hydraulic circuit. the PVT solar field is arranged in two groups of of 10 PVT collectors; within each group, the PVT collectors are hydraulically connected in parallel, and both groups are connected, to each other, in series. To simulate the PVT collectors type 50 b is used, the HP is simulated using type 541, which is activated using a pre-defined schedule. Finally, the inertia tank, that integrates the PVT and HP, is simulated with type 534. The corresponding performance curves provided by the HP manufacturer (Hitachi) were included in type 534's configuration. Other components in the solar and HP hydraulic circuits are the circulation pumps, the air cooler, the hydraulic pipes and valves.

The electrical production from the PVT solar field is sent to the electrical subsystem. The main components in this subsystem are a hybrid inverter (Fronius Gen 24 Plus, 8kW) and the Li-ion batteries (BYD, LVS models). The hybrid inverter manages the electrical production to use it directly to meet the electrical demand, or to store the excess in the batteries for later use. The battery models use LFP (Li-Iron-Phosphate) chemestry, which offers better power density, safety performance and higher lifetime compared to other chemistries available on the market; their round-trip efficiency is 96% and they support a maximum Depth of Discharge (DOD) of 90%.

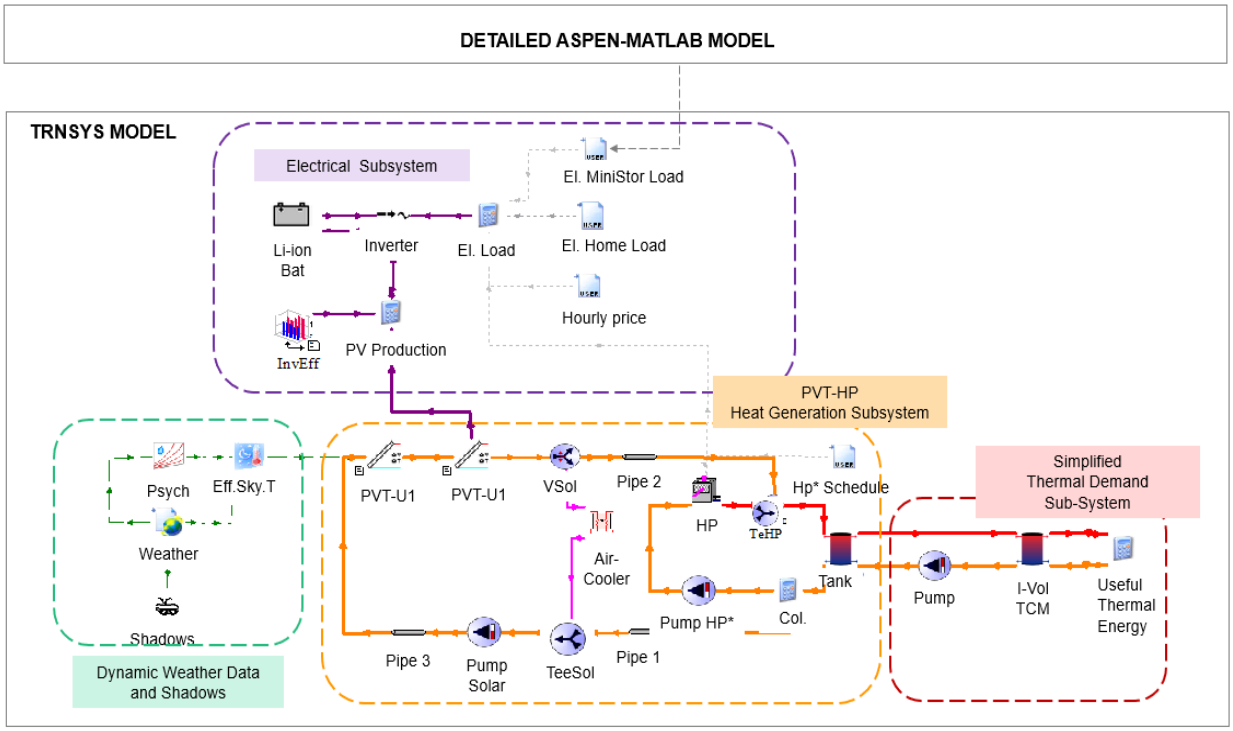

Fig. 2: Model layout implemented in TRNSYS software

To simulate the inverter and batteries types 48b and 47a are used. Additionally, the inverter uses a dynamic efficiency. Considering the previously mentioned battery models, specific commercial sizes (10.24, 12.8, 16.56 and 20.48 kWh) were used to perform a sensitivity analysis to select the optimal battery size.

The electrical subsystem requires as inputs the electrical load profiles for the MiniStor system and the building, which were obtained for typical days as section 2.2 described. Particularly, the electrical load profiles for the MiniStor system were estimated using a detailed ASPEN - MATLAB/Simulink model previously developed (Zisopoulos et al., 2021). These electrical loads were defined for two TCM reactor sizes (30 and 17.5 kWh).

The thermal production from the PVT-HP subsystem is sent to the MiniStor system, represented as a simplified thermal demand subsystem, which includes a hydraulic circuit between the inertia tank and the TCM reactor, a circulation pump to discharge the inertia tank, the inertia volume in the TCM reactor (type 534). The thermal demand of the TCM is simulated in a simplified way using an auxiliary calculation element, assuming a ΔT of 5 °C when the PVT-HP generation system sends thermal energy to the reactor. Table1 summarizes the different types used in the TRNSYS simulation model.

Tab. 1 : Summary of components used in the implemented TRNSYS Model

Subsystem	Component	Type /Library
PVT-HP subsystem	Unglazed PVT Collectors	Type 50b / Standard
	Air-to water HP	Type 941 / TESS
	Inertia tank, Air-cooler	Type 91 / Standard
	Inertia tank	Type 534 /TESS
Electrical subsystem	Hybrid inverter	Type 48b / Standard
	Li-ion batteries	Type 47a / Standard
	Dynamic efficiency hybrid inverter	Type 581 / TESS
Simplified thermal subsystem	Inertia TCM volume	Type 534 Standard
	Circulation pump TCM loop	Type 110 / Standard
	Complementary calculations	Equa
Weather data subsystem	Reading weather and external data	Type 15-3, 9 /Standard

	Psychrometric calculations	Type 33 /TESS
	Sky temperature calculations	Type 69 / Standard

2.4 PVT solar hybrid collector characterization

As stated was stated in the previous section, the simulation model uses a liquid-based unglazed PVT collector. This PVT collector corresponds to a prototype which was characterized in a test rig in accordance with the European Norm EN ISO- 9806 (CEN and CENELEC, 2014) and following the procedure applied in other studies where PVT collectors are also characterized and analysed (Simón-Allué et al., 2022).

$$\eta_{th} = \eta_0(1 - b_u u) - (b_1 + b_2 u)\left(\frac{T_m - T_a}{G^{"}}\right) \qquad \text{(eq. 1)}$$

This standard indicates that the thermal efficiency (η_{th}) for this PVT collector type has a linear behavior, dependent on incident solar radiation, fluid temperature, ambient temperature and wind speed, as Equation 1 indicates, where u corresponds to the wind velocitythe, η_0 represents the optical efficiency of the collector, b_u is a coefficient dependent on wind speed that affects the optical efficiency of the PVT collector; b_1 is the first thermal loss coefficient, and b_2 is the second thermal loss coefficient, also dependent on wind velocity; T_m corresponds to the mean fluid temperature in the PVT collector, T_a is the ambient temperature, $G^{"}$ is the net irradiance.

Tab. 2: Technical characteristics of the PVT solar collector

Description		Unit	Value
General characteristics	Dimensions: Length x Width x Height	[mm]	1719x1140x35
	Gross area	[m^2]	1.96
	Weight	[kg]	22
Main electrical characteristics STC	Cell type	[-]	Si-monocrystalline, PERC
	Efficiency STC (1)	[%]	19.9
	Power at maxim power point (PMPP)	[W]	390
	Temperature NOTC (2)	[°C]	42.3±2
	Power temperature coefficient	[% . K^{-1}]	-0.34%
Main thermal characteristics	Absorber type	[-]	Sheet & tubs
	Absorber materials	[-]	Aluminum and cooper
	Optical efficiency η_0	[-]	0.405
	Coefficient: b_u	[s/m]	0.0175
	First thermal loss coefficient: b_1	[W. m^{-2}. K^{-1}]	8.52
	Second thermal loss coefficient: b_2	[W. s. m^{-3}. K^{-1}]	0.275

(1) STC: Standard Testing Conditions; (2) Normal Operation Temperature Cell

2.5 Performance indicators

A set of performance indicators was defined to assess the effect of battery size on the solar fraction and grid system dependency (Alanne, 2023; IEA, 2023b). The corresponding applied formulation is presented below.

The Solar thermal fraction (SF_{th}) corresponds to the monthly thermal energy produced by the PVT solar field (Q_{PVT}), sent to the inertia tank, divided by the total thermal energy produced by the PVT-HP system (Zenhäusern et al., 2020)., as Equation 2 shows, where Q_{HP} represents the air-source HP thermal production

$$SF_{th} = \frac{Q_{PVT}}{Q_{PVT} + Q_{HP}} \qquad \text{(eq. 2)}$$

Similarly, the solar electrical fraction (SF_{el}) is calculated as the relation between the monthly electricity produced by the PVT solar field (E_{PVT}) divided by the electrical loads (E_L), according to Equation 3. In this case, the electrical loads considered are due to the air-source HP ($E_{L,Hp}$) and the MiniStor system ($E_{L,Ms}$).This solar fraction is assumed to range 0 to 1; therfore, values above 1 were normalized to 1 . Values above 1 means that there is an electricity excess, which can be either stored in the batteries for later use or fed into the grid.

$$SF_{el} = \frac{E_{PVT}}{E_{L,Hp} + E_{l,Ms}} \quad \text{(eq. 3)}$$

To evaluate the influence of the battery size on the electrical grid dependency, the grid fraction (GF) is used, which is calculated as the ratio between the electricity taken from the grid (E_{grid}) and the electrical loads (E_L), using Equation 4. For this indicator, three different scenarios are considered: i) loads due to the air-source HP; ii) loads due to the air-source HP and the MiniStor system; iii) loads due to the air-source HP, the MiniStor system and the building.

$$\mathrm{GF} = \frac{E_{grid}}{E_L} \quad \text{(eq. 4)}$$

3. Results and Discussion

3.1 Annual energy demand

The annual thermal demand in the building is 7940 kWh, with 72% attributable to the heating and the remaining 28%, to DHW. Figure 3 (a) shows the monthly evolution for the thermal demand. During the winter period the demand is higher with monthly values between 793 and 1750 kWh, while during the summer and intermediate seasons the demand decreases drastically with monthly values from 169 to 189 kWh, which are linked exclusively to the DHW.

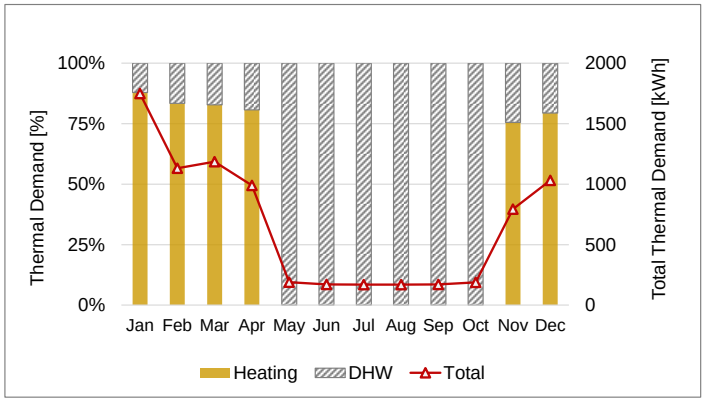

(a) Thermal demand

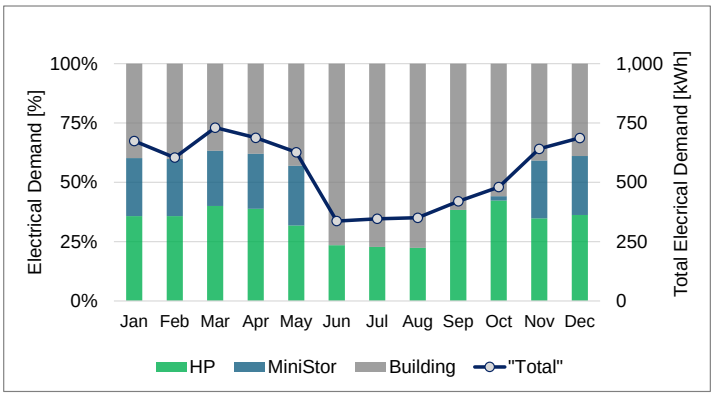

(b) Electrical demand

Fig. 3: Monthly thermal and electrical demand by type of use

Regarding the electrical demand, Figure 3(b) shows the electrical loads by use when the TCM storage has a capacity of 30 kWh. The annual electrical consumption is 6588 kWh, with 48.0% due to the building, 34.8% to the HP and 17.2% to the internal components of the MiniStor system. When the TCM capacity is 17.5 kWh the annual electrical consumption is slight higher (0.35%) with a similar share values by use (47.8% due to the building, 32.2% to the HP and 20% to the MiniStor system). These values indicate that the use of MiniStor system represents a high increment in the electrical demand. Therefore, the system control strategy for the HP and MiniStor system activation is based on a limited schedule, defined according to the electrical production

from the PVT solar field, in order to drive the MiniStor system using mainly renewable energy resources.

3.2 Sensitivity analysis of the battery size on the grid dependency

The sensitivity analysis of battery size on the grid dependency was performed for the two defined TCM storage capacities (30 and 17.5 kWh) and considered four commercial sizes for the ESS (10.24, 12.8, 16.56 and 20.48 kWh). The first TCM capacity (30 kWh) is closer to the daily building heating demand, therefore the Li-ion batteries provide a complementary energy storage capacity to cover the overall building energy demand (electrical and thermal). The second TCM capacity (17.5 kWh) is lower than the daily heating demand, so in this case the Li-ion batteries are focused on also covering the thermal building demand.

To size the electrical batteries as maximum value for the Grid Factor of 0.3 was assumed to limit the system grid dependency, besides SF_{el} above 0.80 on monthly basis were verified once the batteries were sized . Figure 4 shows the results for the three scenarios describe in section 2.5, considering different electrical load profiles during the winter months.

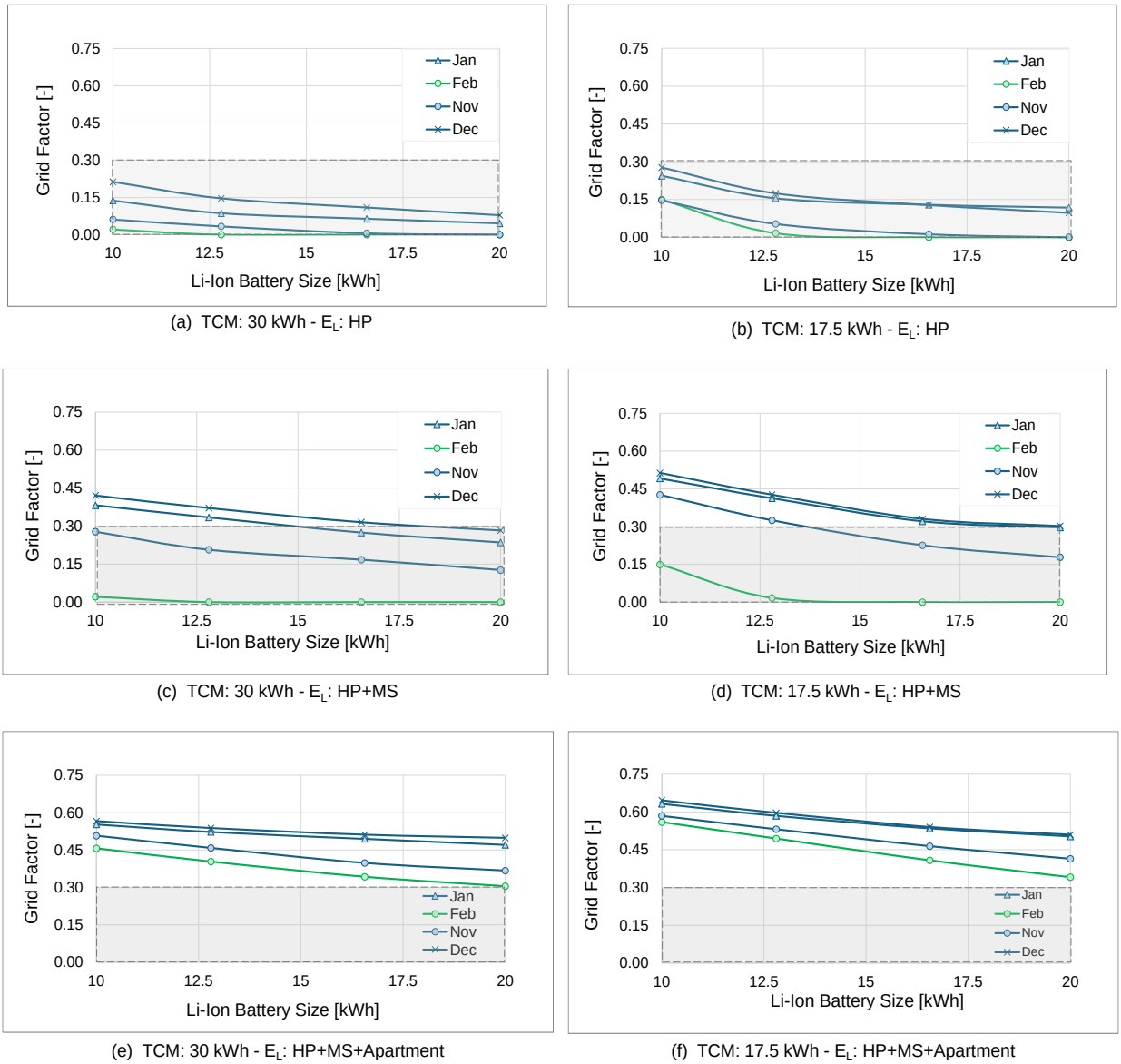

(a) TCM: 30 kWh - E_L: HP

(b) TCM: 17.5 kWh - E_L: HP

(c) TCM: 30 kWh - E_L: HP+MS

(d) TCM: 17.5 kWh - E_L: HP+MS

(e) TCM: 30 kWh - E_L: HP+MS+Apartment

(f) TCM: 17.5 kWh - E_L: HP+MS+Apartment

Fig. 4: Electricity taken from the grid for different energy storage sizes.

The first scenario includes the electrical loads due to the air-source HP (Figures 4.a and 4.b). In this scenario, for all battery sizes, the GF is below the target value. When the electrical battery size has the minimal simulated capacity (10.24 kWh), the maximum monthly value for the GF is 0.21 for the TCM capacity of 30 kWh and 0.28 if the TCM capacity is reduced to 17.5 kWh . Therefore, in this scenario, the grid dependency improves

when the TCM capacity is higher, that indicates a better interaction between the HP electrical load profile and the battery storage.

The second scenario considers the electrical loads due to the HP as well as the MiniStor system (Figures 4.c and 4.d). In this scenario, the GF is close to the target value, when an electrical battery size of 16.56 kWh is considered. Specifically, the GF is 0.32 and 0.33 for the TCM capacities of 30 and 17.5 kWh respectively; therefore, in this scenario, there is not a significant impact on the grid dependency, due to the additional capacity in the TCM.

Finally, the third scenario includes the electrical loads due to the HP, the MiniStor system and the building (Figure 4.e and 4.f). In this scenario, the GF target value is not achieved for any simulated battery size, because the electrical loads due to the building are bigger than loads linked to the HP and MiniStor system. For the maximum simulated battery size (20.48 kWh), the maximum GF values are 0.50 and 0.51 for the TCM capacities of 30 and 17.5 kWh.

Considering the above, when the HP and the MiniStor loads are included (second scenario),, the suitable capacities for the TCM and the electrical storage are 17.5 kWh and 16.56 kWh respectively, since the GF factor associate to these values is close to the target value of 0.30. There is no significant reduction in the GF factor when a higher TCM size is used. The final energy storage sizes must also consider other relevant variables such as the system and electricity costs.

3.3 Solar fractions

This subsection presents the PVT energy production with the solar fractions for the second scenario, using 17.5 and 16.56 kWh sizes for the TCM storage and Li-ion batteries respectively. Regarding the PVT electrical performance (Figure 5.a), the system achieves an annual production of 8732 kWh , which exceeds the overall annual electrical demand by 30%, including the air-source HP, the MiniStor system as well as the building.

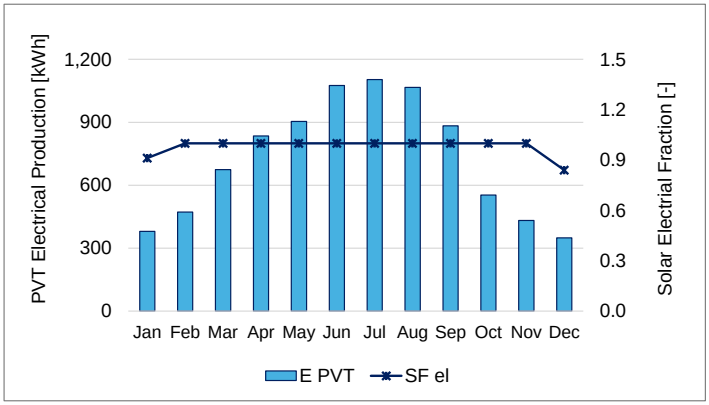

(a) PVT electrical production

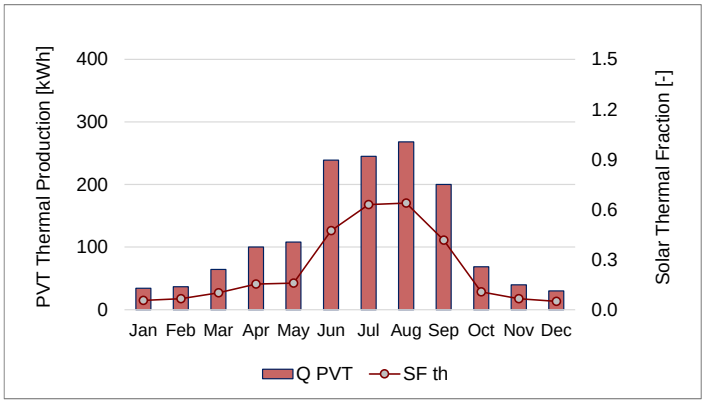

(b) PVT thermal production

Fig. 5: Monthly thermal and electrical demand by type of use.

Considering the HP and the MiniStor loads, the SF_{el} is high throughout the year with a minimal value of 0.84

in December and 0.91 in January; for the rest of the months, this fraction reaches values of 1.0. These high fractions suggest that the GF factor obtained (0.33) could be improved by implementing additional actions based on demand response strategies.

In relation to the PVT thermal performance (Figure 5.b), the annual production is 1434 kWh. The corresponding SF_{th} gets values between 0.06 and 0.11 in winter, so the effective solar thermal contribution to the thermal demand is relatively low in winter. On the contrary, during summer the SF_{th} achieves values between 0.42 and 0.64 indicating a high contribution to the DHW deman . Despite the low SF_{th}in winter, the SF_{el} and the GF show good performance, which guarantees that the MiniStor system will contribute to the thermal building demand using mainly solar energy.

4. Conclusions

The previous analysis revised the grid dependency of the considered energy system, including two types of energy storages (ESS based on Li-ion batteries and thermochemical (TCM)). The results lead to the following main conclusions:

The grid factor, as an indicator, helps to optimally define the sized combination of these two energy storage technologies. For the analyzed system, there is a similar grid factor (0.32 and 0.33) when an ESS of 16.5 kWh is used together with either TCM sizes (30 and 17.5 kWh). To complete the optimization a complementary analysis must be carried out, considering different cost factors such as investment, maintenance, and useful life, as well as other factors such as the availability of materials to manufacture these technologies at local and global levels.

Regarding the solar thermal fraction, the PVT technology achieves higher values in summer than in winter in winter. This performance is mainly due to the high temperature required by the TCM in the MiniStor system and the system's demand in winter. To achieve better performance, other technologies can be evaluated in the overall energy system such glazed PVT as well as solar thermal technology.

The thermal energy produced by the PVT-HP system primarily comes from renewable sources, as the activation of the HP uses a limited schedule linked to the PVT electrical production. Thanks to this control strategy, the system achieves higher solar electrical fractions and lower grid factors to cover the electrical loads for the HP and the MiniStor system.

These grid factors can potentially be improved considering that the solar electrical fraction reaches values above 0.84 on a monthly basis, when the electrical loads include the air-source HP and the MiniStor system. To achieve this improvement the HP activation should be optimized by obtaining a more accurate forecast for the expected PVT electrical production and implementing complementary demand response strategies.

5. Acknowledgments

This paper was prepared in the context of the European Union's Horizon 2020 research and innovation program through grant agreement No 869821 (Minimal Size Thermal and Electrical Energy Storage System for In-Situ Residential Installation - MiniStor). The authors also express their gratitude to the Universidad de Santiago de Compostela for supplying the data required to estimate the thermal and electrical energy demand for the analyzed case.

6. References

Alanne, K., 2023. Study on reducing the grid dependency of urban housing in Nordic climate by hybrid renewable energy systems. Renew. Energy Focus 46, 1–15. https://doi.org/10.1016/j.ref.2023.05.006

CEN, CENELEC, 2017. EN 12831-1 Energy performance of buildings - Method for calculation of the design heat load - Part 1: Space heating load, Module M3-3 18-22+95.

CEN, CENELEC, 2014. Solar energy. Solar thermal collectors -Test methods. EN-ISO 9806:2013.

Dincer, I., Rosen, M.A., 2011. Thermal energy storage. Systems and applications, 2nd ed. Wiley. A John Wiley and Sons, Ltd., UK.

Fan, Y., Luo, L., 2018. Energy Storage by Sensible Heat for Buildings, in: Wang, R., Zhai, X. (Eds.), Handbook of Energy Systems in Green Buildings. Springer, Berlin, Heidelberg. https://doi.org/https://doi.org/10.1007/978-3-662-49088-4_40-1

IEA, 2023a. World Energy Outlook 2023.

IEA, 2023b. Electricity Grids and Secure Energy Transitions. https://doi.org/10.1787/455dd4fb-en

IEA (International Energy Agency), 2022. Solar Thermal Market Records Year of Growth. SOLARUPDATE. Newsl. IEA Solar-Heating Cool. Program. 75, 1–29.

Jarimi, H., Aydin, D., Yanan, Z., Ozankaya, G., Chen, X., Riffat, S., 2019. Review on the recent progress of thermochemical materials and processes for solar thermal energy storage and industrial waste heat recovery. Int. J. Low-Carbon Technol. 14, 44–69. https://doi.org/10.1093/ijlct/cty052

Jouhara, H., Żabnieńska-Góra, A., Khordehgah, N., Ahmad, D., Lipinski, T., 2020. Latent thermal energy storage technologies and applications: A review. Int. J. Thermofluids 5–6, 100039. https://doi.org/10.1016/j.ijft.2020.100039

Kebede, A.A., Kalogiannis, T., Van Mierlo, J., Berecibar, M., 2022. A comprehensive review of stationary energy storage devices for large scale renewable energy sources grid integration. Renew. Sustain. Energy Rev. 159, 112213. https://doi.org/10.1016/j.rser.2022.112213

Koçak, B., Fernandez, A.I., Paksoy, H., 2020. Review on sensible thermal energy storage for industrial solar applications and sustainability aspects. Sol. Energy 209, 135–169. https://doi.org/10.1016/j.solener.2020.08.081

Lazzarin, R., 2020. Heat pumps and solar energy: A review with some insights in the future. Int. J. Refrig. 116, 146–160. https://doi.org/10.1016/j.ijrefrig.2020.03.031

MI (Mordor Intelligence), 2022. Global Enery Storage System Market.

Ministry of Development of Spain, 2019. Technical building Code - Basic Energy Saving Document (CTE-DB-HE). Código Técnico de la Edificación -Documento Básico Ahorro de Energía (CTE-DB-HE).

Salgado-Pizarro, R., Calderón, A., Svobodova-Sedlackova, A., Fernández, A.I., Barreneche, C., 2022. The relevance of thermochemical energy storage in the last two decades: The analysis of research evolution. J. Energy Storage 51. https://doi.org/10.1016/j.est.2022.104377

SEL (Solar Energy Laboratory), 2018. TRNSYS 18 - A Trnsient Syste, Simulation Program. Volume 8 - Weater Data.

Simón-Allué, R., Guedea, I., Coca-Ortegón, A., Villén, R., Brun, G., 2022. Performance evaluation of PVT panel with phase change material: Experimental study in lab testing and field measurement. Sol. Energy 241, 738–751. https://doi.org/10.1016/j.solener.2022.05.035

Tiwari, A.K., Chatterjee, K., Agrawal, S., Singh, G.K., 2023. A comprehensive review of photovoltaic-thermal (PVT) technology: Performance evaluation and contemporary development. Energy Reports 10, 2655–2679. https://doi.org/10.1016/j.egyr.2023.09.043

Tsimpoukis, A., Martinopoulos, G., Nikolopoulos, N., 2024. Analysis of a novel compact integrated thermal energy storage system (MiniStor) in European sites, in: 12th International Conference on Improving Energy Efficiency ICommercial Buildings and SmartCommunities. European Union, pp. 3–14. https://doi.org/10.2760/716916

Xu, Y., Pei, J., Cui, L., Liu, P., Ma, T., 2022. The Levelized Cost of Storage of Electrochemical Energy Storage Technologies in China. Front. Energy Res. 10, 1–16. https://doi.org/10.3389/fenrg.2022.873800

Zenhäusern, D., Gagliano, A., Jonas, D., Tina, G.-M., Hadorn, J.-C., Lämmle, M., Herrando, M., 2020. Key performance indicators for PVT Systems. IEA SHC, Task 60 PVT Systems, Report D1. https://doi.org/10.18777/ieashc-task60-2020-0007

Zisopoulos, G., Nesiadis, A., Atsonios, K., Nikolopoulos, N., Stitou, D., Coca-Ortegón, A., 2021. Conceptual design and dynamic simulation of an integrated solar driven thermal system with thermochemical energy storage for heating and cooling. J. Energy Storage 41. https://doi.org/10.1016/j.est.2021.102870

Zondag, H.A., 2008. Flat-plate PV-Thermal collectors and systems: A review. Renew. Sustain. Energy Rev. 12, 891–959. https://doi.org/10.1016/j.rser.2005.12.012